

## Supplementary Information

# Preparation of silicate nanosheet by delaminating RUB-18 for transparent, proton conducting membranes.

Keisuke Awaya,<sup>a</sup> Kazutoshi Sekiguchi,<sup>b</sup> Hirotake Kitagawa,<sup>b</sup> Shuhei Yamada,<sup>b</sup> Shintaro Ida<sup>a</sup>

a) Institute of Industrial Nanomaterials (IINa), Kumamoto University; Chuo-ku, Kumamoto, 860-8555, Japan.

b) Materials Research Laboratories, Nissan Chemical Corporation; Funabashi, Chiba, 274-0052, Japan.

### **Materials**

Tetrabutylammonium hydroxide ((C<sub>4</sub>H<sub>9</sub>)<sub>4</sub>N<sup>+</sup>OH<sup>-</sup>, 10% in water), methanol (99.7%), ethanol (99.5%), 1-propanol (99.5%), tert-butanol (100%), nitric acid (60%), and 5% Nafion<sup>TM</sup> dispersion solution were purchased from Fujifilm Wako Pure Chemical Corporation. 2-propanol (99.5%) was purchased from Nacalai Tesque, Inc. 46.3% Pt/C powder was purchased from Tanaka Kikinzoku Kogyo. Sodium silicate solution was provided by Nissan Chemical Corporation. Toray carbon paper EC-TP1-060T was purchased from Toyo Corporation. A Pt/C ink was prepared from a mixture of 46.3% Pt/C, 5% Nafion dispersion, 2-propanol, and deionised water.

### **Synthesis of protonated RUB-18 (H-RUB-18)**

The layered silicate RUB-18 was synthesised according to previously used methods.<sup>S1-S2</sup> First, 2400 g of aqueous sodium silicate solution (SiO<sub>2</sub>/Na<sub>2</sub>O molar ratio of 3.7, or 22.8 wt% SiO<sub>2</sub> and 6.4 wt.% Na<sub>2</sub>O) was poured into a stainless-steel autoclave (SUS316, 3000 cm<sup>3</sup>) and was heated at 383 K for 12 d to produce Na-RUB-18. The precipitate was filtered and rinsed with water, and then dried at 313 K. Protonated Na-RUB-18 (H-RUB-18) was prepared by ion-exchange of the interlayer sodium ions by protons in 0.1 M HNO<sub>3</sub> (1 g per 200 mL) for 30 min with stirring, followed by immersion in the acid for 24 h without stirring. Finally, the precipitate was filtered, rinsed with water, and dried at 313 K.

### **Delamination of H-RUB-18**

Typically, 30 mg of H-RUB-18 was added to 20 mL of 0.05 M tetrabutylammonium hydroxide (TBAOH) in methanol–water mixtures (0–100 vol.% methanol content). A 50 vol.% mixture was prepared to investigate the thermal durability, proton conductivity, and to produce the free-standing membrane, which was ultrasonicated at 240 W for 18 h. The dispersion was centrifuged at 2000 rpm for 30 min, and the supernatant was used for further investigations.

### **Preparation of a freeze-dried silicate nanosheet**

The silicate nanosheet dispersion was centrifuged at 12000 rpm for 60 min. The supernatant was removed, and the precipitate was dispersed in tert-butanol. The final dispersion was cooled to ~223 K at ~10 Pa for 2 d.

### **Preparation of a spin-coated silicate film**

Delamination was performed using the same method with 150 mg of H-RUB-18 and a 50 vol.% methanol–water mixture. The dispersion was centrifuged at 2000 rpm for 30 min, and ~20 mL of the supernatant was added to 20 mL of methanol. The spin-coating process was performed on a Si wafer (9 cm<sup>2</sup>) with the following steps: 1) 200 rpm/5 s, 2) 0 rpm/3 s, and 3) 2000 rpm/5 s. The spin-coated samples were annealed at 473, 673, 873, or 1073 K for 1 h (10 K/min).

### **Preparation of a free-standing silicate nanosheet membrane**

The silicate nanosheet dispersion was centrifuged at 12000 rpm for 60 min, and the precipitate was dispersed in methanol (1.1 mg/mL). The final dispersion was vacuum filtered using a polycarbonate (PC) membrane filter with a pore size of 0.2 μm. After drying at room temperature, the silicate nanosheet membrane (diameter: ~18 mm) was detached from the PC membrane filter.

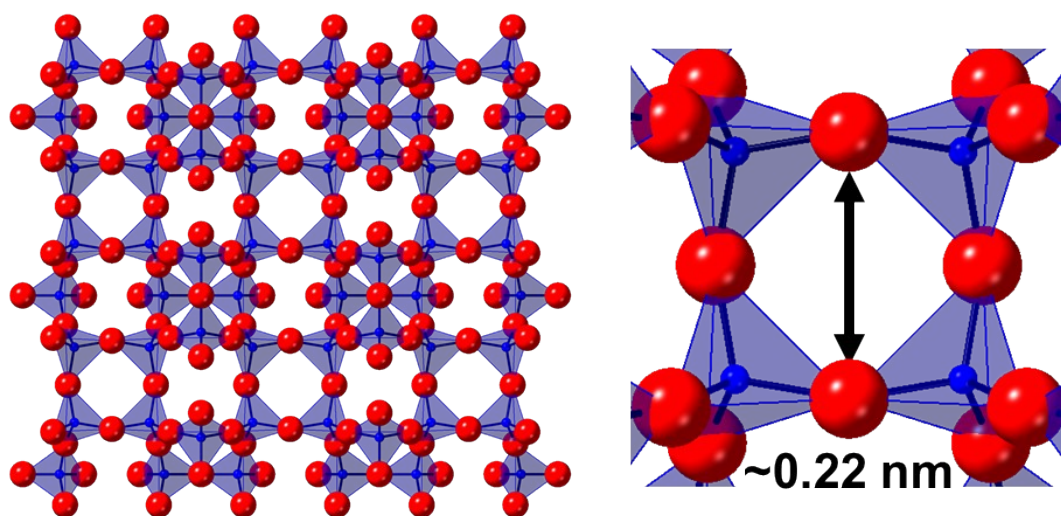
### **Preparation of a free-standing graphene oxide-silicate nanosheet-graphene oxide membrane**

The dispersion of graphene oxide was prepared by the modified Hummers' method.<sup>S3-S4</sup> Firstly, the dispersion of graphene oxide was filtered using the same PC membrane filter for the silicate nanosheet membrane. After drying the graphene oxide membrane, the silicate nanosheet dispersion was added on the membrane. Finally, the graphene oxide dispersion was added on the dried graphene oxide-silicate nanosheet membrane. The dried membrane was detached from the PC membrane filter and was used as a graphene oxide-silicate nanosheet-graphene oxide membrane.

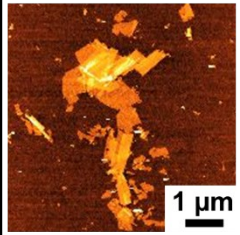
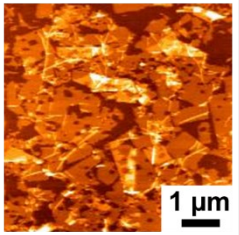
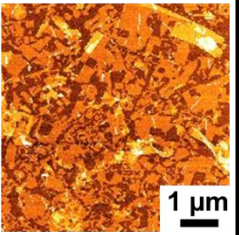
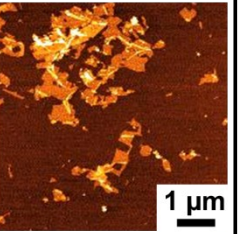
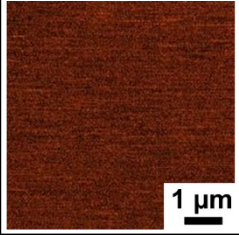
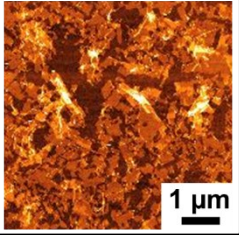
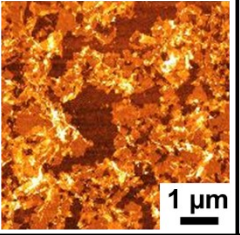
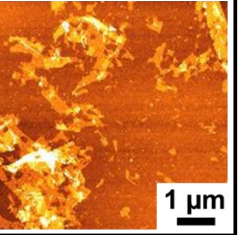
### **Characterization**

X-ray diffraction (XRD) patterns were obtained using a SmartLab X-ray diffractometer (Rigaku Corporation) with a CuKα X-ray source ( $\lambda = 0.15418$  nm) with a Kβ cut filter. Atomic force microscopy (AFM) images of the silicate nanosheet were obtained using a Nanoscope instrument (Hitachi High-Tech Corporation) in tapping mode with a Si single-crystal cantilever. The freeze-dried silicate nanosheets and the free-standing silicate nanosheet membrane were imaged using a field emission scanning electron microscope (FE-SEM, SU8000, Hitachi High-Tech Corporation) and SEM (JSM-6000LV, JEOL Ltd.). Raman spectra were obtained using an NRS-3100 instrument (JASCO Corporation). High-angle annular dark-field scanning transmission electron microscopy (HAADF-STEM) and energy dispersive X-ray spectroscopy (EDS) images of the silicate nanosheets were obtained using a Tecnai instrument (Thermo Fisher Scientific) equipped with an EDAX module. The Brunauer–Emmett–Teller (BET) surface area of the freeze-dried silicate nanosheets was obtained using a Tristar II 3020 surface area and porosity measurement system with N<sub>2</sub> gas (Micromeritics Instrument Corporation). The proton conductivity of the silicate nanosheet in Figure S8 was evaluated using a Solartron SI1260 impedance spectrometer (Toyo Corporation) over a frequency range from  $1 \times 10^6$  to  $5 \times 10^{-3}$  Hz. The silicate nanosheet dispersion was dropped onto a Pt interdigitated array (IDA) electrode (comb interval: 2 μm, No. 012258, BAS Inc.) for impedance measurements. The thickness of the silicate was 1.6 μm, which the value was used for calculating the proton conductivity. The relative humidity (40–98% RH) and temperature (303–343 K) were controlled by an SH-221 Bench-Top Type

Temperature & Humidity Chamber (ESPEC Corp.) and ETTAS EO300E (AS ONE Corporation). The PCM fuel cell test was performed using a Pem Master PEM-004 (Chemix Co., Ltd.) at 353 K with 20 sccm of H<sub>2</sub> and O<sub>2</sub> gas flow. <sup>29</sup>Si dipole decoupling nuclear magnetic resonance (<sup>29</sup>Si DD NMR, 9.4 T, 79.4 MHz resonance frequency) spectra were recorded using a JNM-ECZ400R system (JEOL Ltd.), where 950 scans were accumulated with 60 s of relaxation delay. The samples were packed in 4-mm zirconia rotors (spinning rate: 10 kHz).



**Figure S1.** Ball and stick models of the crystal structure of a single silicate layer of RUB-18 along [001] direction.

		Volumetric alcohol contents in the alcohol-water mixture			
		87 %	50 %	25 %	10 %
Alcohol species	Ethanol $C_2H_5OH$				
	2-Propanol $C_3H_7OH$				

**Figure S2.** AFM images showing the silicate nanosheets delaminated in alcohol-water mixtures with 10-87 vol.% contents of alcohol (ethanol or 2-propanol).

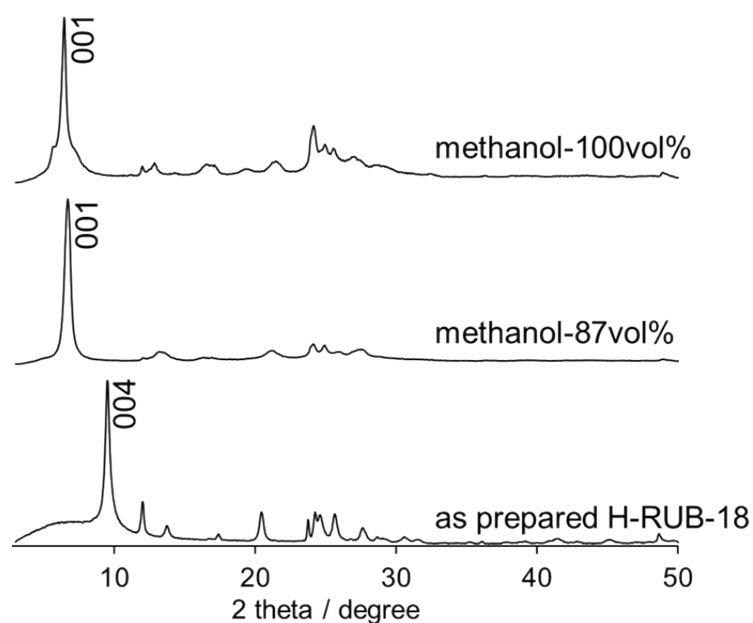


**Figure S3.** Powder XRD patterns ( $2\theta/\theta$  scan) of as prepared H-RUB-18 and precipitates obtained after the ultrasonication treatment in 87 vol.% and 100 vol.% of methanol.

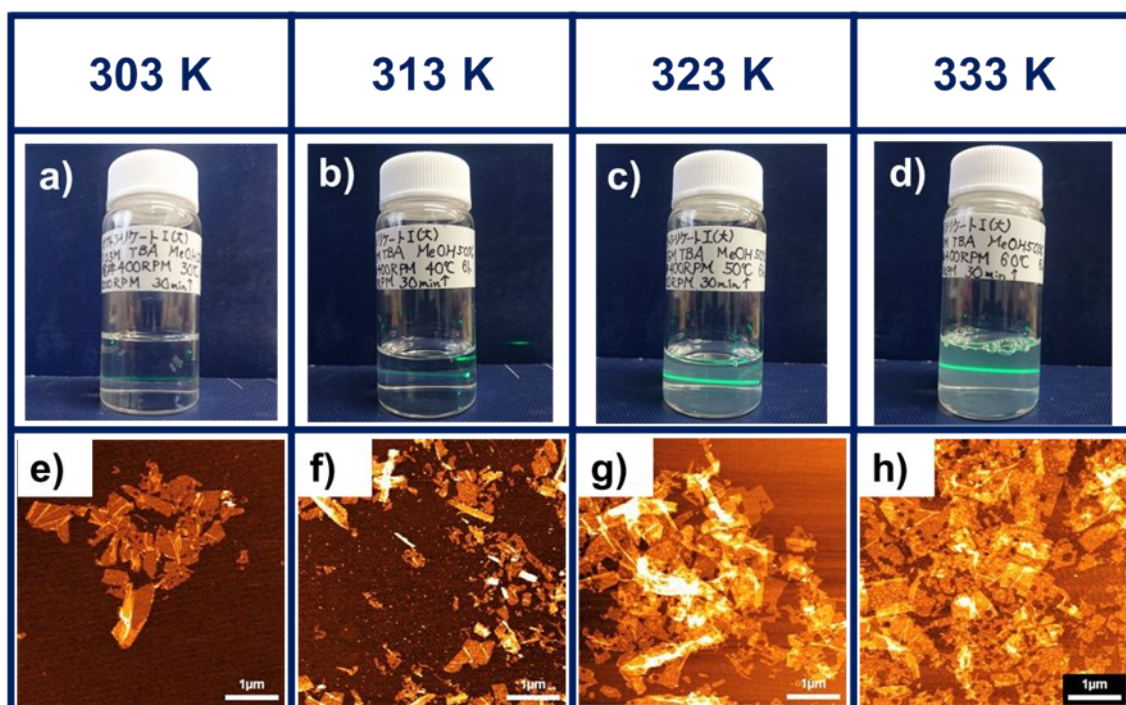


**Figure S4.** (a-d) Photographs of the dispersion of the silicate nanosheet and (e-h) AFM images of the silicate nanosheet. The delamination process was performed in 50 vol.% methanol at 303-343 K with 400-rpm stirring for 6 h.

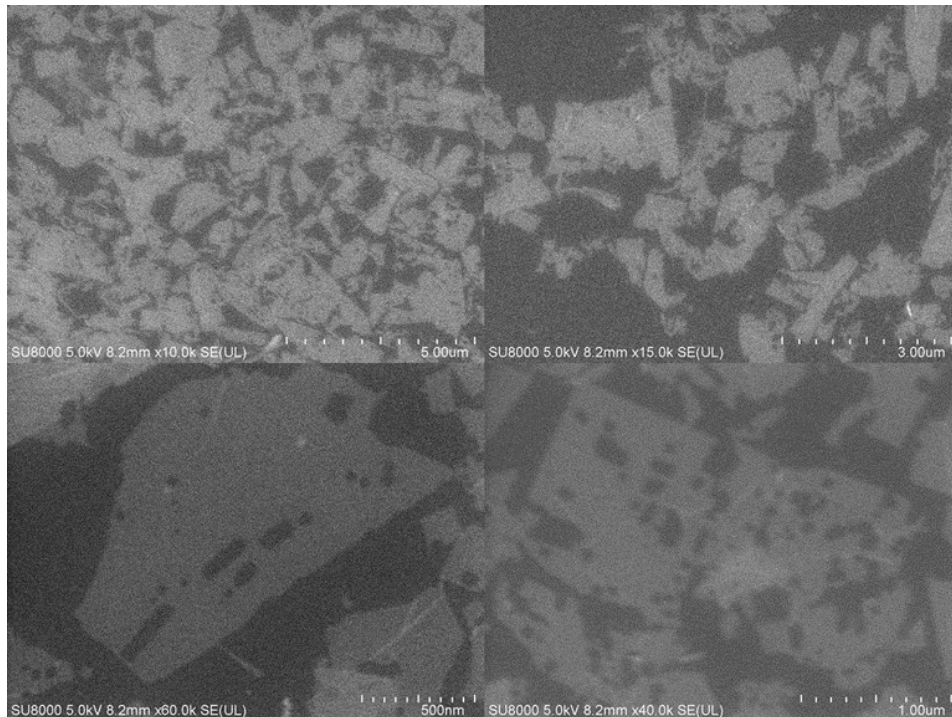


**Figure S5.** FE-SEM images of the silicate nanosheet on Si wafer.

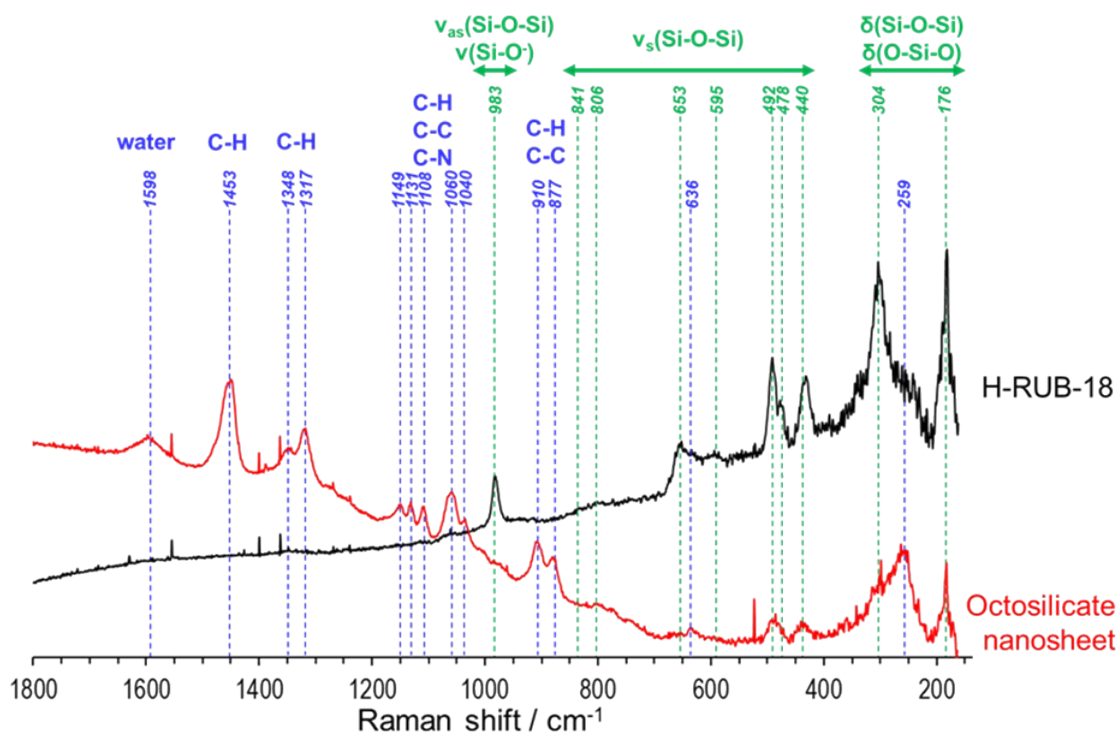


**Figure S6.** Raman spectra of the H-RUB-18 and the freeze-dried silicate nanosheet.

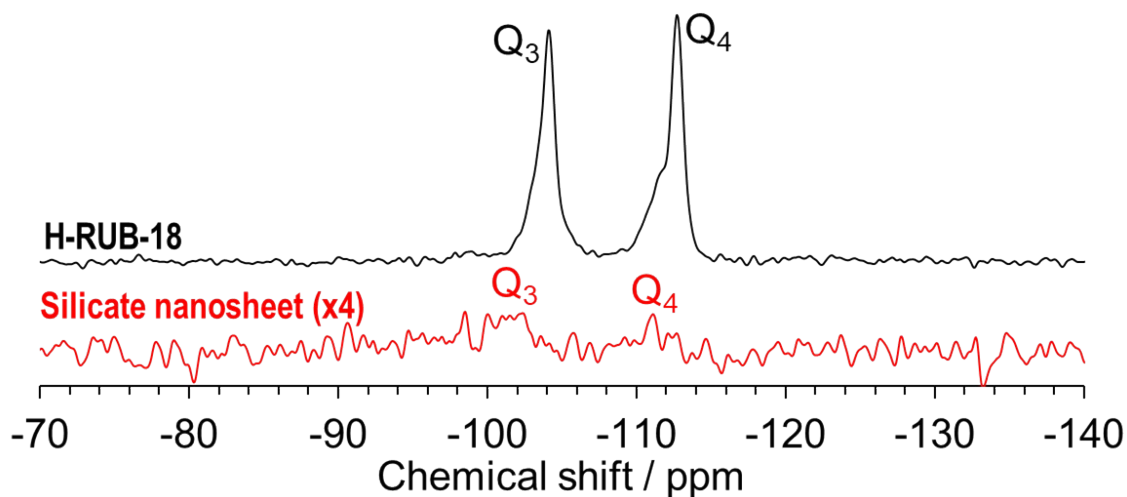


**Figure S7.**  $^{29}\text{Si}$  DD NMR spectra of the H-RUB-18 and the freeze-dried silicate nanosheet.



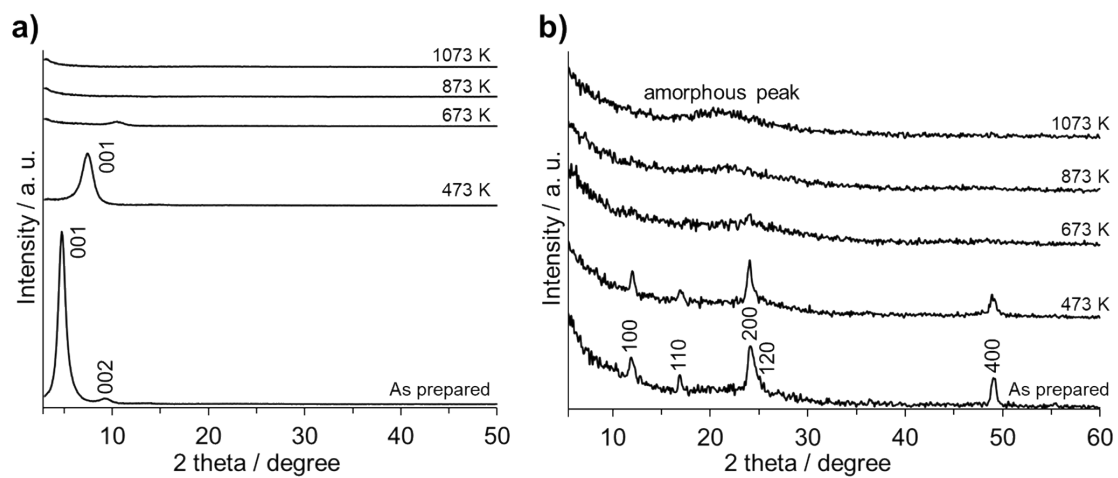


**Figure S8.** Out-of-plane XRD patterns ( $2\theta$  scan) and (d) in-plane XRD patterns ( $2\theta/\phi$  scan) of the spin coating of the silicate nanosheet before and after annealing treatment at 473-1073 K.



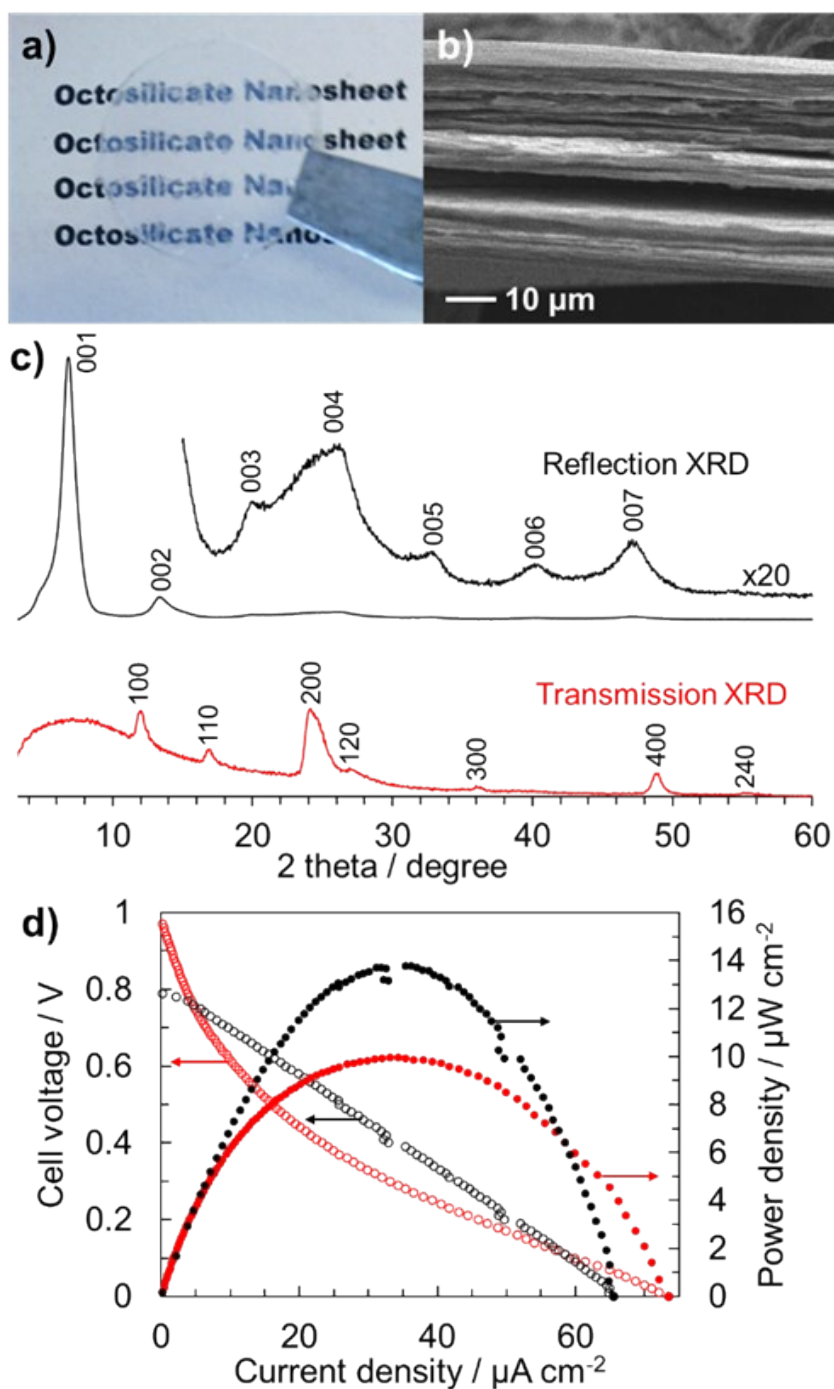


**Figure S9.** (a) a photograph showing the free-standing silicate nanosheet membrane. (b) a SEM image of the cross-sectional view of the free-standing silicate nanosheet membrane. (c) reflection and transmission XRD ( $2\theta/\theta$  scan) patterns of the free-standing silicate nanosheet membrane. (d) cell voltage/power density-current density curves of the free-standing silicate nanosheet membrane (black plots) and graphene oxide-silicate nanosheet-graphene oxide membrane (red plots) obtained from the proton conducting membrane fuel cell (PCMFC) measurement.

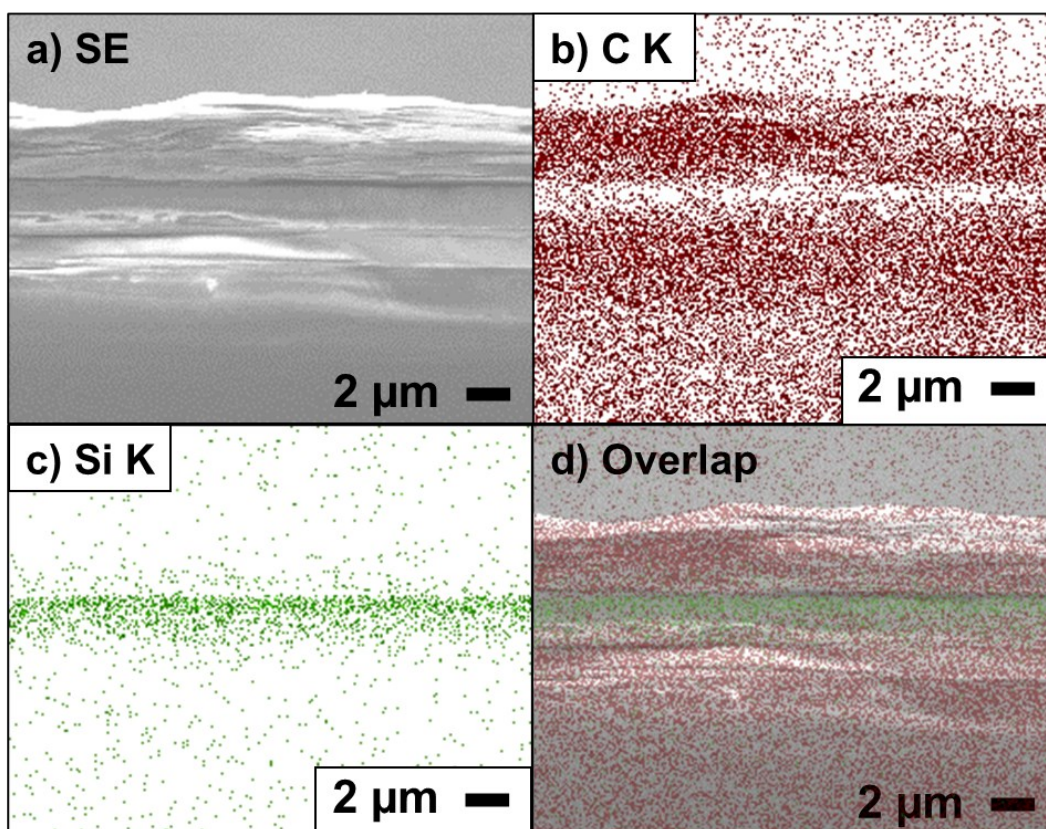


**Figure S10.** FE-SEM and EDS mapping images of a cross-sectional view of GO-silicate NS-GO membrane. (a) SEM, (b) O K, (c) Si K EDS mapping, and an (d) overlapped image of (a-c).

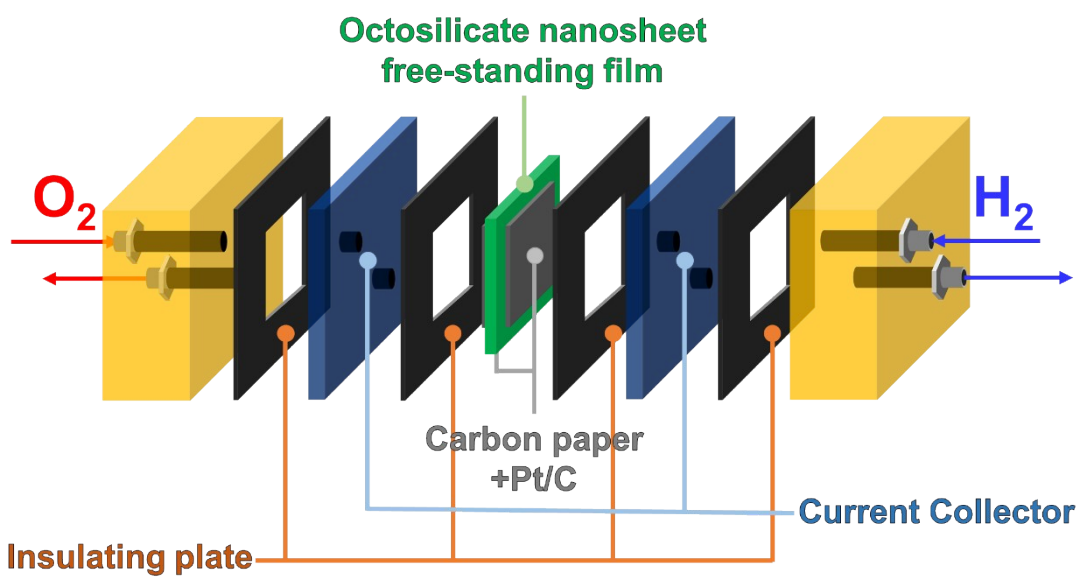


**Figure S11.** Schematic illustration showing a configuration of the proton conducting membrane fuel cell (PCMFC).

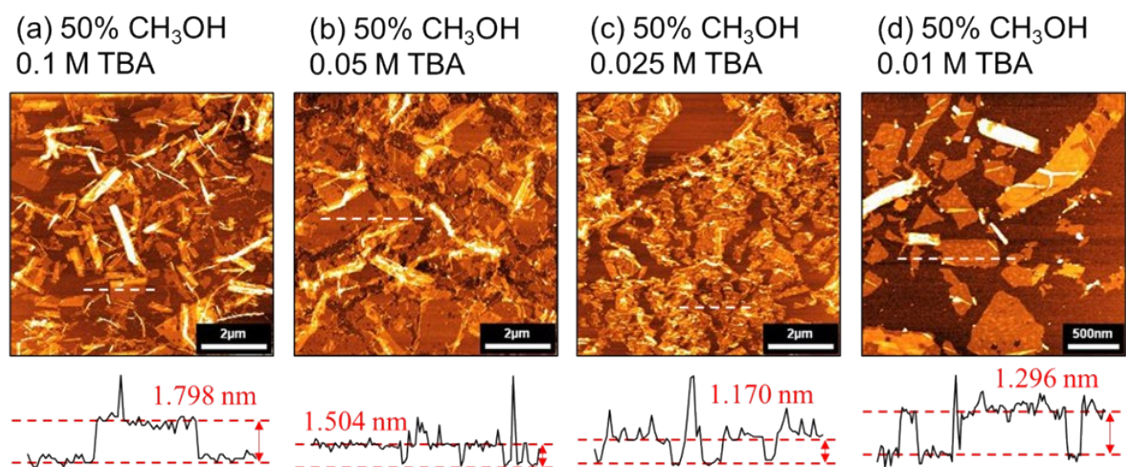


**Figure S12.** AFM images of the silicate nanosheet delaminated in 0.1, 0.05, 0.025, 0.01 M TBAOH in 50 vol.% methanol.

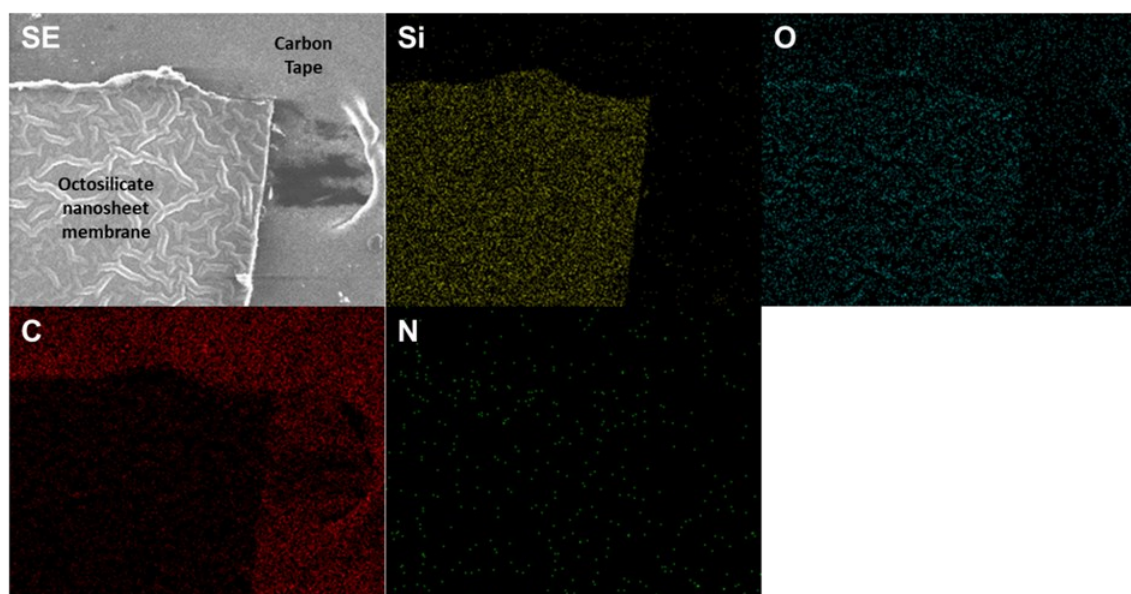


**Figure S13.** FE-SEM image and SEM-EDS mapping images for Si K, O K, C K, N K of the free-standing silicate nanosheet membrane on a carbon tape.

## **References**

- S1)** G. Borbély, H. K. Beyer, H. G. Karge, W. Schwieger, A. Brandt, K. -H. Bergk, Chemical Characterization, Structural Features, and Thermal Behavior of Sodium and Hydrogen Octosilicate, *Clays Clay Miner.* **1991**, 39, 490-497.
- S2)** T. Ikeda, Y. Oumi, T. Takeoka, T. Yokoyama, T. Sano, T. Hanaoka, Preparation and crystal structure of RUB-18 modified for synthesis of zeolite RWR by topotactic conversion, *Microporous Mesoporous Mater.* **2008**, 110, 488-500.
- S3)** N. I. Zaaba, K. L. Foo, U. Hashim, S. J. Tan, W. -W. Liu, C. H. Voon, Synthesis of Graphene Oxide using Modified Hummers Method: Solvent Influence, *Procedia Eng.* **2017**, 184, 469-477.
- S4)** M. R. Karim, M. S. Islam, K. Hatakeyama, M. Nakamura, R. Ohtani, M. Koinuma, S. Hayami, Effect of Interlayer Distance and Oxygen Content on Proton Conductivity of Graphite Oxide. *J. Phys. Chem. C* **2016**, 120, 21976-21982.